

## Structural damage alarming and localization of cable-supported bridges using multi-novelty indices: a feasibility study

Yi-Qing Ni<sup>\*1</sup>, Junfang Wang<sup>1a</sup> and Tommy H.T. Chan<sup>2b</sup>

<sup>1</sup>*Department of Civil and Environmental Engineering, The Hong Kong Polytechnic University, Hung Hom, Kowloon, Hong Kong*

<sup>2</sup>*School of Civil Engineering and Built Environment, Queensland University of Technology, Brisbane, Australia*

*(Received November 30, 2014, Revised February 7, 2015, Accepted February 18, 2015)*

**Abstract.** This paper presents a feasibility study on structural damage alarming and localization of long-span cable-supported bridges using multi-novelty indices formulated by monitoring-derived modal parameters. The proposed method which requires neither structural model nor damage model is applicable to structures of arbitrary complexity. With the intention to enhance the tolerance to measurement noise/uncertainty and the sensitivity to structural damage, an improved novelty index is formulated in terms of auto-associative neural networks (ANNs) where the output vector is designated to differ from the input vector while the training of the ANNs needs only the measured modal properties of the intact structure under in-service conditions. After validating the enhanced capability of the improved novelty index for structural damage alarming over the commonly configured novelty index, the performance of the improved novelty index for damage occurrence detection of large-scale bridges is examined through numerical simulation studies of the suspension Tsing Ma Bridge (TMB) and the cable-stayed Ting Kau Bridge (TKB) incurred with different types of structural damage. Then the improved novelty index is extended to formulate multi-novelty indices in terms of the measured modal frequencies and incomplete modeshape components for damage region identification. The capability of the formulated multi-novelty indices for damage region identification is also examined through numerical simulations of the TMB and TKB.

**Keywords:** structural health monitoring; damage alarming and localization; multi-novelty indices; auto-associative neural networks; cable-supported bridges

---

### 1. Introduction

Maintaining the safe and reliable operation of vital infrastructure systems that society depends upon is critical to securing the well-being of people, protecting significant capital investments, and supporting the vitality of regional economy. However, infrastructure systems cannot last forever; even after construction, these complex systems begin to deteriorate within the demanding operational environment in which they are placed. Given the costs associated with infrastructure

---

\*Corresponding author, Professor, E-mail: [ceyqni@polyu.edu.hk](mailto:ceyqni@polyu.edu.hk)

<sup>a</sup>Research Fellow

<sup>b</sup>Professor

repair and the high environmental impact of infrastructure construction, government authorities worldwide are increasingly seeking sensing and instrumentation systems to more objectively monitor crucial infrastructure systems to ensure structural and operational safety. Structural health monitoring (SHM) technology can provide engineers and asset managers with early warnings on damage and structural deterioration prior to the need for costly repairs or situations that can lead to catastrophic structural collapses. The past two decades have witnessed a rapid increase in the applications of SHM technology to various civil engineering structures around the world (Aktan *et al.* 2001, DeWolf *et al.* 2002, Ko and Ni 2005, Brownjohn 2007, Catbas 2009, Fujino *et al.* 2009, Glisic *et al.* 2009, Ni *et al.* 2009a, Ou and Li 2009, Wang and Yim 2010, Ni *et al.* 2011, Yun *et al.* 2011, Ye *et al.* 2013, Dan *et al.* 2014, Teng *et al.* 2015).

In Hong Kong, a sophisticated long-term SHM system, named “Wind And Structural Health Monitoring System (WASHMS)” has been devised by the Highways Department of Hong Kong SAR Government and implemented on the suspension Tsing Ma Bridge (TMB), the cable-stayed Kap Shui Mun Bridge (KSMB), and the cable-stayed Ting Kau Bridge (TKB) in the late 1990s (Lau *et al.* 1999, Wong 2004). This on-line system consists of about 800 permanently installed sensors, including strain gauges, accelerometers, displacement transducers, anemometers, temperature sensors, level sensors, weigh-in-motion sensors, and global positioning systems (GPS). The implementation of this SHM system highlights the necessity of developing practical damage detection methodologies for large-scale civil structures. A research team from The Hong Kong Polytechnic University was commissioned by the Highways Department of Hong Kong SAR Government to investigate the feasibility of using the measured dynamic characteristics from the system to detect structural damage in the three instrumented bridges (Ko *et al.* 1999, 2000, 2002, 2009). The feasibility study indicates that because of very low modal sensitivity of the structures with respect to damage at a component level, only the methods which have high tolerance to incompleteness of measured data, measurement noise, modeling error and structural uncertainty are applicable to large-scale cable-supported bridges for vibration-based damage detection.

Among a variety of vibration-based damage detection methods developed in the past two decades, the novelty detection technique has been demonstrated to be greatly promising for damage occurrence detection of structures in operation with noisy measurement data (Worden 1997, Chan *et al.* 1999, Sohn *et al.* 2002, Sim *et al.* 2004, Yan *et al.* 2004, Oh *et al.* 2009, Zhou *et al.* 2011b). The novelty detection technique, in the context of unsupervised learning paradigm, requires neither structural model nor damage model in both training and testing phases; it is therefore applicable to structures of arbitrary complexity. Also, it is intrinsically tolerant of uncertainties inherent in in-service structures caused by varying operational and environmental conditions. As a drawback, this technique usually requires a sequence of measurements; but it is not a problem for a structure instrumented with an online SHM system. Worden (1997) formulated a novelty measure in terms of the auto-associative neural network (ANN) with its input and output being the system transmissibility for fault detection of a simulated mechanical system. Chan *et al.* (1999) proposed an ANN-based novelty index constructed using measured modal frequencies for anomaly detection of bridge cables. Sohn *et al.* (2002) used the coefficients from an autoregressive and autoregressive with exogenous input (AR-ARX) model to construct an ANN-based novelty detector for structural damage identification under changing environmental and operational conditions. Sim *et al.* (2004) proposed an adaptive novelty detector initially to distinguish between normal and damaged conditions, and later to distinguish between known and unknown damage states. Yan *et al.* (2004) constructed a Kalman model by performing a stochastic subspace

identification to fit the measured response time-history of the healthy structure and employed the residual error between the prediction by the identified model and the actual response measurement from an unknown state of the structure as a novelty detector for damage diagnosis. Oh *et al.* (2009) employed the kernel principal component analysis in conjunction with generalized extreme value statistics for statistical novelty detection of the hangers in a suspension bridge. With the intention of avoiding false-positive and false-negative alarms, Zhou *et al.* (2011b) studied the environment-tolerant capacity of an ANN-based novelty detector purposed for structural damage detection by incorporating generalization techniques in training the ANN and proposed a probability-based procedure to determine the alarming threshold. It is worth mentioning that while being tolerant of uncertainties caused by environmental variability and measurement error, the ANN-based novelty detection technique may fail to discriminate between the detected anomaly resulting from structural damage and resulting from sensor fault. Some recent investigations on sensor validation with sensor fault and distinguishing between sensor fault and structural damage are available (Abdelghani and Friswell 2007, Hernandez-Garcia and Masri 2008, Kullaa 2010, 2011). The potential false-positive alarm caused by a significant variation in environmental effects can be alleviated by embedding a monitoring-derived environmental effect model into the novelty detection technique (Zhou *et al.* 2011a).

In the current formulation of novelty detectors in terms of ANNs, the input and output vectors to train the ANN are the same sequence of measurements from the healthy structure; and the ANN is forced to learn just the significant prevailing features of the patterns inherent in the measurement data through a special design of the neural network architecture with a ‘bottleneck’ hidden layer. In addition, the existing novelty detectors can only accomplish the detection of damage occurrence. In the present study, an improved novelty index is formulated in an effort to enhance the tolerance to measurement noise/uncertainty and the sensitivity to structural damage. In this new formulation, the output vector is designated to differ from the input vector; but the training of the ANN still only needs a sequence of measurements from the intact structure under varying operational and environmental conditions. The enhanced capability of the improved novelty index will be validated through numerical simulation conducted on a free side-span main cable on the TMB, where a comparison of the anomaly detection results by the conventional and improved novelty indices is provided. The damage detectability of the improved novelty index formulated using only modal frequencies will be examined through simulation studies by considering diverse damage scenarios on the TMB and TKB. Then the improved novelty index will be extended to formulate multi-novelty indices in terms of modal frequencies and incomplete modeshape components for damage region identification. The capability of the formulated multi-novelty indices for damage region identification will be verified through numerical simulations of the TMB and TKB.

## 2. An improved novelty index

### 2.1 Formulation

A novelty detector can be realized by constructing an ANN that is configured as a multi-layer perceptron with ‘bottleneck’ hidden layer(s) (Rumelhart *et al.* 1986, Hinton 1989, Petsche *et al.* 1996, Worden 1997, Chan *et al.* 1999). As shown in Fig. 1, the ANN is trained to reproduce at the output layer, the patterns which are presented at the input layer. Thus the output layer must have

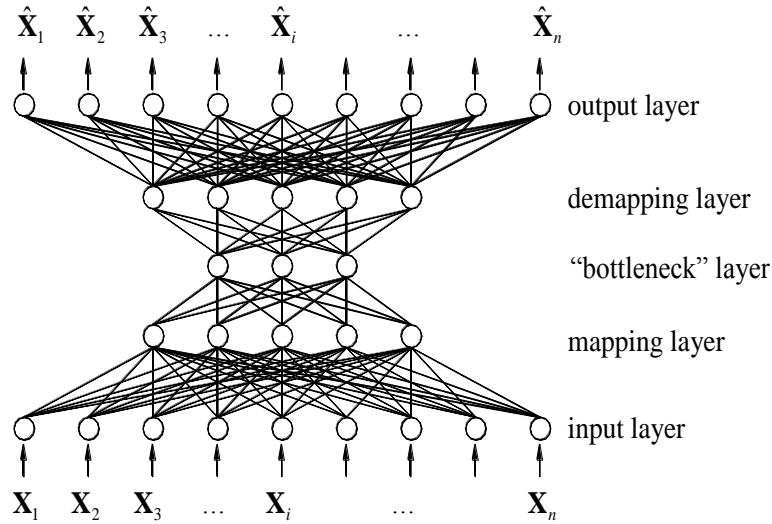


Fig. 1 Auto-associative neural network (ANN)

the same number of the input nodes. However, the input values will not be perfectly reconstructed in the output since the patterns are passed through the hidden layer which has fewer nodes than the input layer. The network is forced to learn just the significant prevailing features of the input patterns. After the network being trained, the input data presented on training are passed again into the trained network to yield a set of output data. The difference between the input and output vectors is measured using some form of distance function, called *novelty index*. In the testing phase, a new series of measurement data obtained later from an unknown state of the structure (damaged or undamaged) is fed into the above network to form a novelty index sequence of testing phase. If this sequence deviates from the novelty index sequence of training phase, the occurrence of damage is alarmed.

When the ANN technique is used for structural damage or anomaly detection, a series of measurement data or measurement-derived quantities (e.g., modal parameters) from the healthy intact structure under normal operational and environmental variations,  $\mathbf{X} = \{X_1, X_2, \dots, X_n\}^T$ , is used to train the ANN. It is worth noting that each entry  $X_i$  ( $i=1, 2, \dots, n$ ) in  $\mathbf{X}$  denotes a set of measured/identified quantities of a physical parameter (e.g., the frequency for the  $i$ th mode) obtained from the healthy structure under varying operational and environmental conditions. No information on the structural model is needed. In the current practice of configuring the ANN, the data sequence  $\mathbf{X}$  is used as both input vector and output vector to train the ANN; and after performing the training, the data sequence presented on training is fed again into the trained ANN to generate an output sequence  $\hat{\mathbf{X}} = \{\hat{X}_1, \hat{X}_2, \dots, \hat{X}_n\}^T$ . Due to the pinching in the hidden layer of the ANN, only the significant features of the input patterns will progress forward to the output layer; and therefore the output sequence  $\hat{\mathbf{X}}$  is different from the input sequence  $\mathbf{X}$ . Thus the novelty index sequence in the training phase, when using the Euclidean distance, can be obtained as

$$\lambda(\mathbf{X}) = \|\mathbf{X} - \hat{\mathbf{X}} + \delta\| = (\mathbf{X} - \hat{\mathbf{X}} + \delta)^T (\mathbf{X} - \hat{\mathbf{X}} + \delta) \quad (1)$$

where  $\delta$  is a constant and is taken as unity in the present study.

In the testing phase, a new series of measurement data or measurement-derived quantities from an unknown state of the structure (damaged or undamaged),  $\mathbf{X}_t = \{X_{1t} X_{2t} \dots X_{nt}\}^T$ , is obtained. It is passed into the above trained ANN to yield an output sequence  $\hat{\mathbf{X}}_t$ . Then the novelty index sequence in the testing phase is obtained as

$$\lambda(\mathbf{X}_t) = \|\mathbf{X}_t - \hat{\mathbf{X}}_t + \delta\| \tag{2}$$

and a shift of the novelty index sequence between the training phase and the testing phase signals the damage/anomaly presence in the structure.

Eqs. (1) and (2) represent the conventional definition of the novelty index. In the present study, an improved novelty index is formulated in which the output vector in ANN is designated to differ from the input vector. The output vector of the ANN,  $\mathbf{Y} = \{Y_1 Y_2 \dots Y_n\}^T$ , is defined as

$$Y_i = (X_i - m_i)\alpha + m_i \quad (i = 1, 2, \dots, n) \tag{3}$$

where  $m_i$  is the mean of the  $i$ th entry  $X_i$  of the input vector  $\mathbf{X}$  over the training data;  $\alpha$  is a penalty factor to make a tradeoff between enhancing the significant features and amplifying the uncertainty effect. Although the output vector  $\mathbf{Y}$  differs from the input vector  $\mathbf{X}$ , both require only a series of measurement data or measurement-derived quantities from the healthy structure under normal conditions. After training the ANN with  $\mathbf{X}$  and  $\mathbf{Y}$ , the input sequence  $\mathbf{X}$  is fed again into the trained ANN to yield an output sequence  $\hat{\mathbf{Y}}$ , and the novelty index sequence for the training phase is obtained in terms of the Euclidean distance as

$$\lambda(\mathbf{Y}) = \|\mathbf{Y} - \hat{\mathbf{Y}}\| \tag{4}$$

When a new series of measurement data or measurement-derived quantities from an unknown state of the structure (damaged or undamaged),  $\mathbf{X}_t = \{X_{1t} X_{2t} \dots X_{nt}\}^T$ , is obtained, it is passed into the above trained network to yield an output sequence  $\hat{\mathbf{Y}}_t$ . The corresponding novelty index sequence for the testing phase is obtained by

$$\lambda(\mathbf{Y}_t) = \|\mathbf{Y}_t - \hat{\mathbf{Y}}_t\| \tag{5}$$

where  $\mathbf{Y}_t = \{Y_{1t} Y_{2t} \dots Y_{nt}\}^T$  is a vector with its  $i$ th entry being

$$Y_{it} = (X_{it} - m_i)\alpha + m_i \quad (i = 1, 2, \dots, n) \tag{6}$$

If the novelty index sequence in the testing phase deviates from that in the training phase, the occurrence of structural damage/anomaly is flagged; if they are indistinguishable, no damage is signaled.

The role of the penalty factor  $\alpha$  in Eqs. (3) and (6) can be expounded by substituting Eq. (3) into Eq. (4), that is

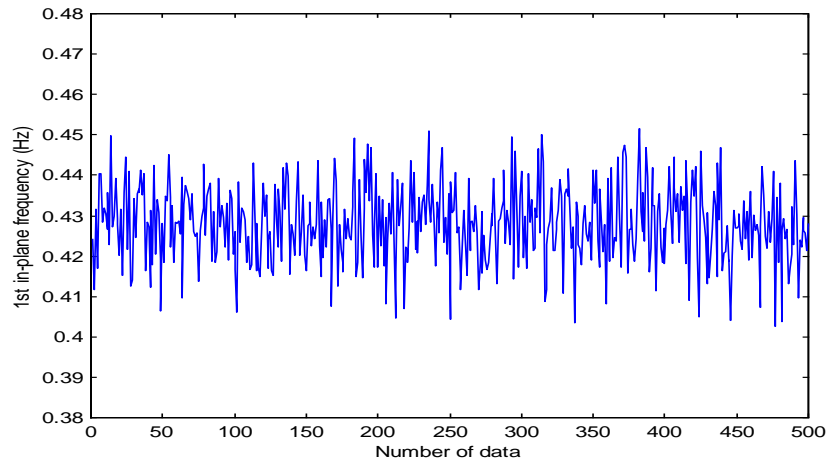
$$\lambda(\mathbf{Y}) = \|\mathbf{Y} - \hat{\mathbf{Y}}\| = \|\mathbf{X} - \hat{\mathbf{X}} + (\alpha - 1)[(\mathbf{X} - \mathbf{m}) - (\hat{\mathbf{X}} - \hat{\mathbf{m}})]\| \tag{7}$$

In the training phase for the intact structure, it is expected that  $\hat{\mathbf{m}}$  is very close to  $\mathbf{m}$  because of the identical input vectors and therefore Eq. (7) approximately generates  $\alpha$  times as from Eq. (1)

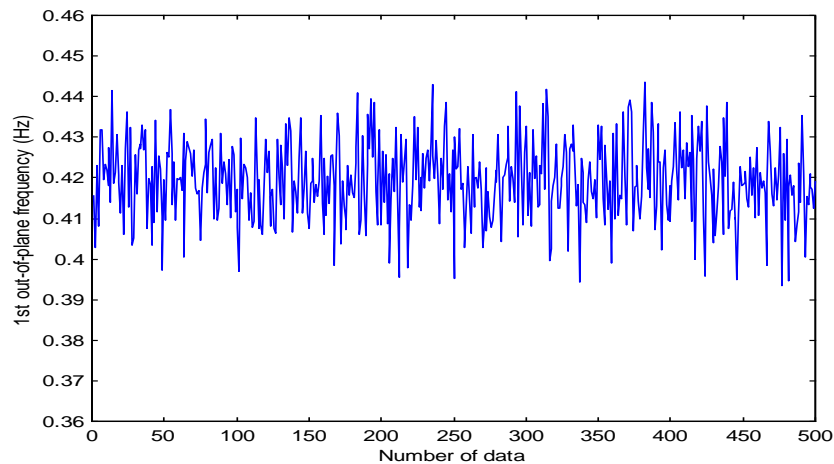


Table 1 Modal frequencies of Tsing Yi side span cable (Hz)

Mode No.	1st	2nd	3rd	4th	5th	6th
In-plane mode	0.4286	0.8424	1.2704	1.7054	2.1517	2.6120
Out-of-plane mode	0.4200	0.8425	1.2701	1.7055	2.1517	2.6120



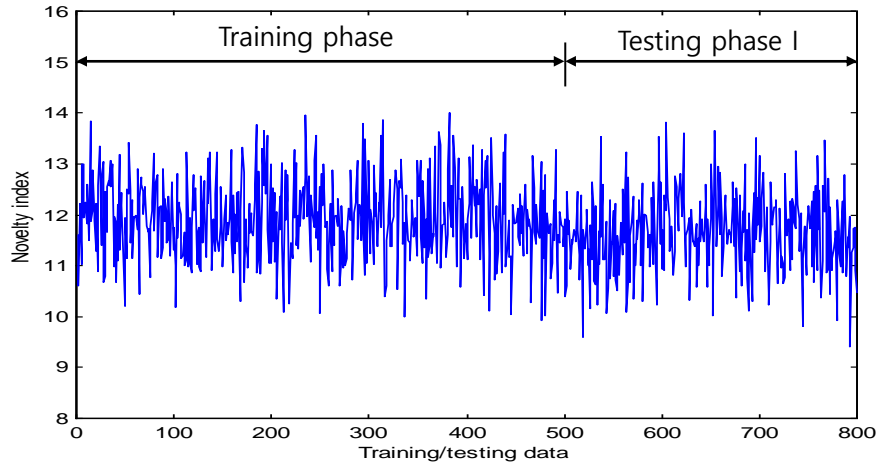
(a) Modal frequency sequence for the 1st in-plane mode



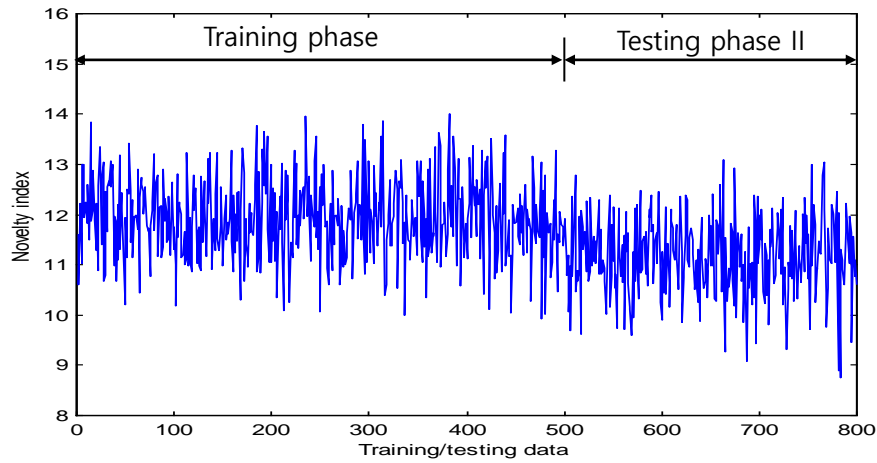
(b) Modal frequency sequence for the 1st out-of-plane mode

Fig. 3 Noise-corrupted modal frequencies of the cable in healthy state

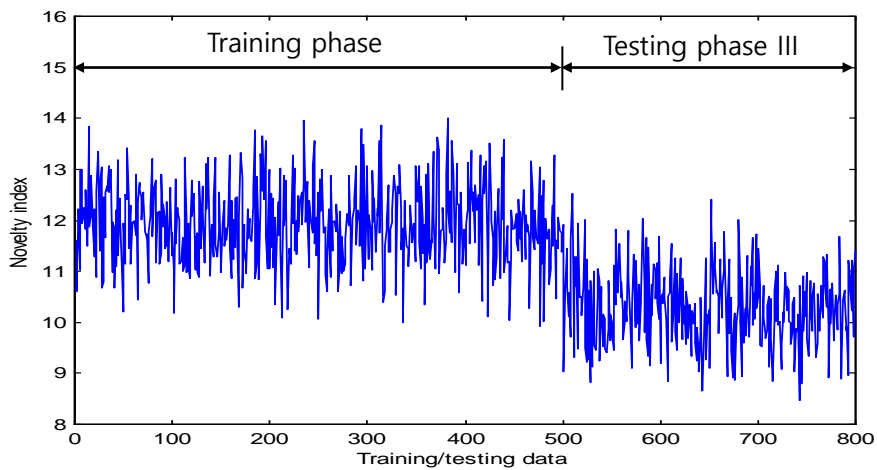
flexural rigidity, sag-extensibility, spatial variability of dynamic tension, boundary conditions, lumped masses and intermediate supports and/or dampers has been developed (Ni *et al.* 2002). It is used in the present study to generate the simulation data for anomaly detection of a freely suspended main cable on the Tsing Yi side span of the TMB. The designated horizontal tension force of the main cables on the Tsing Yi side span is 405,838 kN for each, which is considered as the true tension force in healthy state. The corresponding in-plane and out-of-plane modal frequencies of each cable can be accurately calculated by the above method. Table 1 lists the



(a) Testing data with 2% reduction in cable tension force

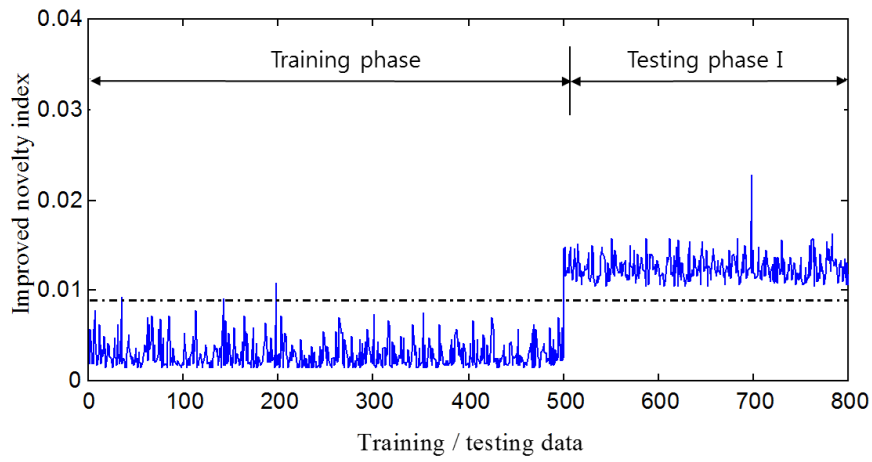


(b) Testing data with 5% reduction in cable tension force

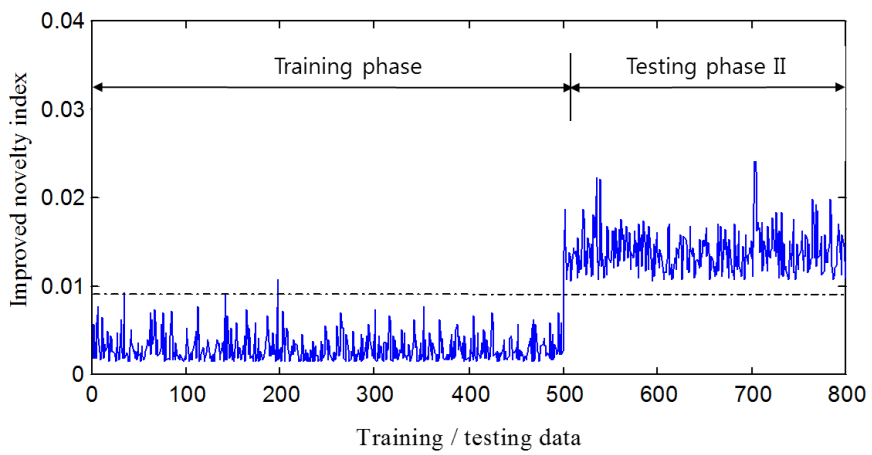


(c) Testing data with 10% reduction in cable tension force

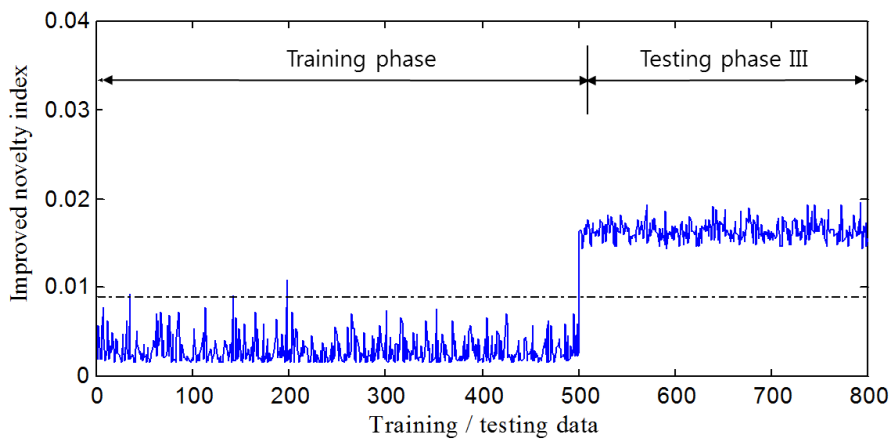
Fig. 4 Original novelty index evaluated on training and testing data



(a) Testing data with 2% reduction in cable tension force



(b) Testing data with 5% reduction in cable tension force



(c) Testing data with 10% reduction in cable tension force

Fig. 5 Improved novelty index evaluated on training and testing data

calculated modal frequencies for the first six in-plane modes and out-of-plane modes.

To account for the measurement error/noise and structural uncertainty due to varying operational and environmental conditions, the ‘identified’ modal frequency sequences of the cable in healthy state are generated by adding to the true tension force a normally distributed random sequence with zero mean and 0.05 variance and then calculating the corresponding modal frequencies at each sample value of the fluctuating tension force. Fig. 3 shows such obtained modal frequency sequences for the first in-plane and out-of-plane modes of the cable in healthy state. The noise-corrupted ‘identified’ modal frequency sequences, each consisting of 500 data samples, for the first six in-plane and out-of-plane modes of the cable in healthy state constitute the input sequence  $\mathbf{X}$  in the training phase ( $\mathbf{X}$  embraces 12 modal frequency elements in column, each having 500 data samples in row).

Two ANNs are then trained with the noise-corrupted ‘identified’ modal frequency sequences in healthy state: the first one is trained by taking  $\mathbf{X}$  as both input and output vectors to the ANN; and the second one is trained by using  $\mathbf{X}$  as input vector and  $\mathbf{Y}$  (calculated from  $\mathbf{X}$  by Eq. (3)) as output vector to the ANN. Both ANNs are configured with a node structure of 12-8-8-12. The activation functions are taken as the tan-sigmoid function between the second and third layers and the linear transfer function between the input and second layers and between the third and output layers. The coefficient  $\alpha$  is taken as 3 in the present study. After performing the training, the data sequence  $\mathbf{X}$  presented on training is fed again into the two trained ANNs to yield the output sequences  $\hat{\mathbf{X}}$  and  $\hat{\mathbf{Y}}$ , respectively; and the novelty index sequences in the training phase,  $\lambda(\mathbf{X})$  and  $\lambda(\mathbf{Y})$ , are then obtained according to Eqs. (1) and (4), respectively.

To examine and compare the ability of the trained ANNs for anomaly detection, the cable tension is reduced by 2%, 5% and 10%, respectively, to simulate three abnormal conditions of the cable. By adding to each of the reduced tension forces a normally distributed random sequence with the same variance (0.05), the noise-corrupted ‘identified’ modal frequency data of the cable corresponding to the three abnormal conditions are generated. The modal frequencies of the twelve modes (the first six in-plane modes and the first six out-of-plane modes) are obtained and each data sequence is generated with 300 data. These ‘identified’ data are taken as new input vectors,  $\mathbf{X}_t$ , which are passed into the above trained ANNs to yield output vectors  $\hat{\mathbf{X}}_t$  and  $\hat{\mathbf{Y}}_t$ . The novelty index sequences in the testing phase,  $\lambda(\mathbf{X}_t)$  and  $\lambda(\mathbf{Y}_t)$ , are then obtained by Eqs. (2) and (5).

Figs. 4 and 5 show the novelty index sequences in both training and testing phases obtained by the two ANNs for the three abnormal cases. For the case with a 2% reduction in cable tension force, the conventional novelty index (Fig. 4(a)) fails to detect the anomaly because the novelty index sequences are not distinguishable between the training and testing phases; whereas, the improved novelty index (Fig. 5(a)) clearly signals the anomaly by a distinct deviation of the novelty index sequence from the training phase to the testing phase. The conventional novelty index ambiguously indicates the anomaly in the case with a 5% reduction in tension force (Fig. 4(b)) and distinctly alarms the anomaly in the case with a 10% reduction in tension force (Fig. 4(c)). When the improved novelty index is used, the anomaly in both cases is unambiguously flagged (Figs. 5(b) and 5(c)), validating the enhanced capability of the improved novelty index for anomaly detection.

### 3. Structural damage alarming by improved novelty index

### 3.1 Suspension Tsing Ma Bridge (TMB)

As the conventional modeling procedure for cable-supported bridges by approximating the bridge deck as analogous continuous beams or grids is incompetent for accurate damage simulation studies, a precise 3D finite element model (FEM) consisting of 17,677 elements and 7,375 nodes has been developed using the commercial ABAQUS software for modal analysis and damage detection simulation studies of the TMB. The developed FEM has the following features: (i) the spatial configuration of the original structure remains in the model; (ii) the geometric stiffness of cables and hangers stemming from the large deflection has been accurately accounted for in the model through a nonlinear static iteration analysis; and (iii) the mass and stiffness contribution of individual structural members is independently described in the model such that the sensitivity of global and local modal properties to any structural member can be evaluated conveniently and accurately. Consequently, damage to any structural member can be directly and precisely simulated. Modal analysis with the FEM indicates that the modal frequencies of the first 67 modes of the TMB are less than 1.0 Hz. The vibration modes of the TMB can be classified into the following categories: (i) global vertical bending modes, (ii) global lateral bending and torsional modes, (iii) central span cable local sway modes, (iv) Ma Wan side span cable local sway modes, (v) Tsing Yi side span free cable local modes (in-plane and out-of-plane), (vi) Ma Wan side span deck dominated modes, and (vii) tower dominated modes (sway, bending and torsion).

The above classification gives guidance to construct ANNs for damage alarming. After merging categories (iv) and (v) into one group and merging categories (vi) and (vii) into one group, five ANNs configured in terms of the improved novelty index are generated for damage occurrence detection of the TMB: the 1st ANN with a node structure 11-6-6-11 has its input layer being the modal frequencies of the first 11 global vertical bending modes (category (i)); the 2nd ANN with a node structure 11-6-6-11 as well has its input layer being the modal frequencies of the first 11 global lateral bending and torsional modes (category (ii)); the 3rd ANN with a node structure 17-9-9-17 has its input layer being the modal frequencies of the first 17 local sway modes of central span cables (category (iii)); the 4th ANN with a node structure 12-6-6-12 has its input layer being the modal frequencies of the first 4 local sway modes of Ma Wan side span cables and the first 8 local sway modes of Tsing Yi side span free cables (categories (iv) and (v)); and the 5th ANN with a node structure 9-5-5-9 has its input layer being the modal frequencies of the first 3 Ma Wan side span deck dominated modes and the first 6 tower dominated modes (categories (vi) and (vii)). It should be noted that the optimal configuration of a multilayer perceptron neural network targeting to maximize its prediction capability can be determined by dividing the training data into training and validation data sets and applying an appropriate regularization technique (Ni *et al.* 2009b). However, the ANNs formulated herein are purposed to retain auto-associative memory instead of prediction capability. By specifying the hidden layers with fewer nodes than the input and output layers, the ANNs are forced to compress redundancies in the input pattern while retaining prevailing features to the output. In the present study, the number of hidden nodes is empirically taken to be approximately half the input and output nodes.

The computed modal frequencies from the FEM are added with normally distributed random noises with zero mean and 0.005 variance (about  $\pm 1.5\%$  maximum error) to form a series of noisy/uncertain 'measured' data (500 data) of the healthy structure which are used to train the five ANNs and obtain the novelty index sequences in the training phase. Then a total of fifteen damage cases, as listed in Table 2, are considered in the simulation study to examine the performance of the improved novelty index for damage occurrence detection. By incurring the assumed damage in

Table 2 Simulated damage cases for TMB

Case No.	Description
1	Damage of one bottom-chord (vertical) bearing at the Ma Wan tower
2	Damage of one side-support (horizontal) bearing at the Ma Wan tower
3	Damage of two side-support (horizontal) bearings at the Ma Wan tower
4	10% reduction in the cross-sectional area of one Ma Wan side span cable
5	0.5 m shift of one Ma Wan anchorage
6	0.05 m slip of one saddle at the top of the Ma Wan tower
7	0.05 m slip of two saddles at the top of the Ma Wan tower
8	Damage of the top cross-beam of the Ma Wan tower
9	Damage of two hangers on the north side near the mid-span
10	Damage of two hangers on the south side near the mid-span
11	Damage of two longitudinal bottom chords near the mid-span
12	Damage of two bottom and two top chords near the mid-span
13	Damage of two diagonal chords near the mid-span
14	Damage of two bottom, two top and two diagonal chords near the mid-span
15	Damage of two parallel rail waybeam sections near the mid-span

the FEM, the modal frequencies for each damage case are calculated. They are then corrupted by normally distributed random noises with zero mean and 0.005 variance to generate the ‘measured’ data in different damage cases. By feeding these new data into the trained ANNs, the novelty index sequence in the testing phase can be obtained for each case. If this sequence deviates from the novelty index sequence in the training phase, the occurrence of damage is alarmed.

Figs. 6 and 7 show the novelty indices for Case 5 and Case 6 evaluated on the five ANNs. To facilitate judgment on the deviation between the training and testing phases, a threshold is also provided in the figures (dotted line). It is defined as  $\delta_\lambda = \bar{\lambda} + 4\sigma_\lambda$  where  $\bar{\lambda}$  and  $\sigma_\lambda$  are the mean and standard deviation of the novelty index sequence over the training data. In Case 5, the novelty index sequences between the testing and training phases are just distinguishable (the deviation between the two phases is visually observable but less than the threshold) when evaluated on the 1st, 3rd and 4th ANNs. When evaluated on the 2nd ANN, the novelty index sequence in the testing phase deviates significantly from the sequence in the training phase, unambiguously signaling the occurrence of damage (the deviation is larger than the threshold). When evaluated on the 5th ANN, the damage occurrence cannot be flagged because the novelty index sequences between the testing and training phases are indistinguishable. In Case 6, the novelty index sequences in the testing phase deviate significantly from the training phase when evaluated on all the five ANNs, unambiguously signaling the damage occurrence. It is found that in the noise level of 0.005 variance ( $\pm 1.5\%$  maximum error), the novelty index fails to indicate the occurrence of damage in Cases 1, 9, 10 and 15. For the damage at deck members (Cases 11 to 14), the novelty index is able to detect the occurrence of damage only when the damage occurs at two top chords, two bottom chords and two diagonal members simultaneously (Case 14). In Cases 2, 3, 7 and 8, the novelty index clearly indicates the damage occurrence. In Case 4, the novelty index sequences between the testing and training phases are just distinguishable. Table 3 summarizes the performance of the five ANNs in damage occurrence detection for all fifteen cases.

It is interesting to relate the damage detectability by means of the novelty index with the level

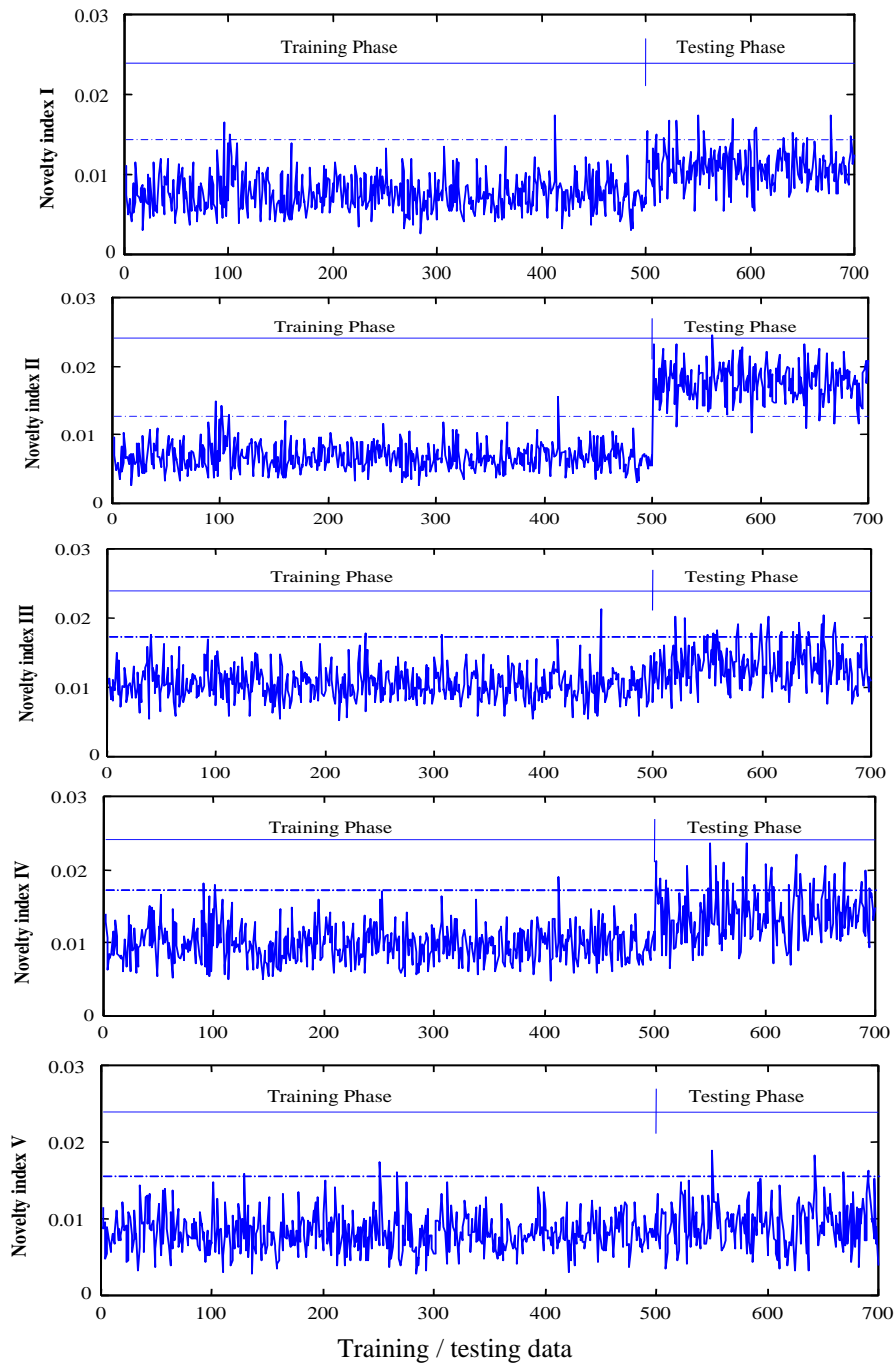


Fig. 6 Novelty index evaluated on the testing data in Case 5 of TMB

of modal frequency change ratios caused by damage. Table 4 lists the evaluated maximum frequency change ratios of the first 60 modes of the bridge corresponding to the fifteen damage cases. It is found that when the maximum frequency change ratio  $\gamma$  is less than 0.3% (Cases 1, 9,

10, 11, 12, 13 and 15), the damage occurrence cannot be flagged by the proposed novelty index. This is because the maximum frequency change ratios in these damage cases are far less than the noise level ( $\pm 1.5\%$  maximum error). When the maximum frequency change ratio  $\gamma$  is between 0.3% and 1.0% (Cases 4 and 14), the damage is just detectable with a weak alarming signature (the

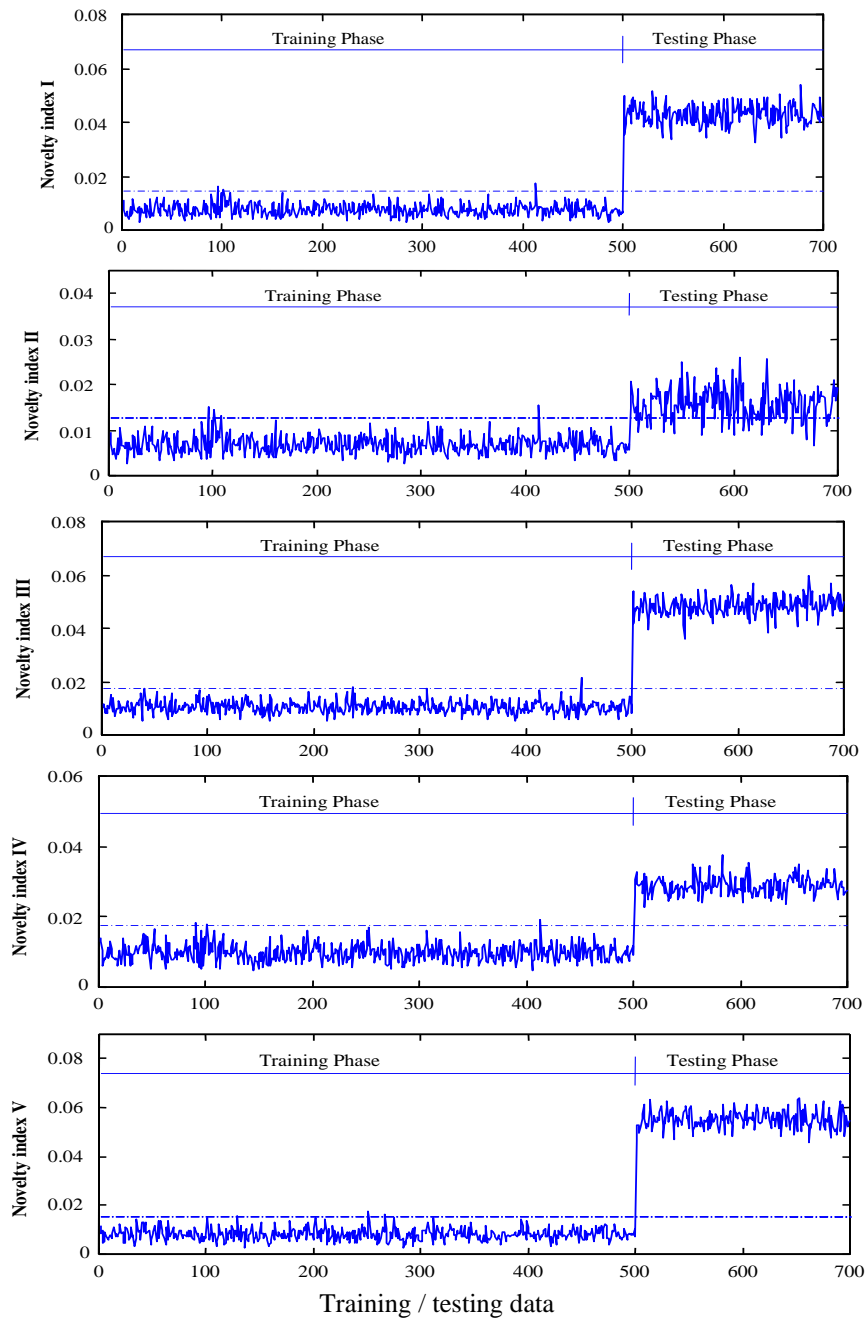


Fig. 7 Novelty index evaluated on the testing data in Case 6 of TMB

Table 3 Structure of ANNs for TMB and damage detection results

ANN No.	Input and output vectors	Node structure	Damage cases successfully detected
I	11 modal frequencies of category (i)	11-6-6-11	Cases 5, 6, 7, and 8
II	11 modal frequencies of category (ii)	11-6-6-11	Cases 2, 3, 5, 6, 7 and 8
III	17 modal frequencies of category (iii)	17-9-9-17	Cases 2, 3, 4, 5, 6, 7, 8 and 14
IV	4 modal frequencies of category (iv) and 8 modal frequencies of category (v)	12-6-6-12	Cases 2, 3, 4, 5, 6, 7 and 8
V	3 modal frequencies of category (vi) and 6 modal frequencies of category (vii)	9-5-5-9	Cases 2, 3, 6, 7, 8 and 14

Table 4 Damage-caused maximum frequency change ratio for TMB

Case No.	Case 1	Case 2	Case 3	Case 4	Case 5
$\gamma$ (%)	0.0873	2.3773	3.0048	0.4556	1.4968
Case No.	Case 6	Case 7	Case 8	Case 9	Case 10
$\gamma$ (%)	3.5823	7.2066	1.8622	0.0786	0.0672
Case No.	Case 11	Case 12	Case 13	Case 14	Case 15
$\gamma$ (%)	0.1688	0.2030	0.0693	0.8843	0.2037

deviation is less than the threshold). The novelty index can unambiguously alarm the damage states when the maximum frequency change ratio  $\gamma$  is greater than 1.0% (Cases 2, 3, 5, 6, 7, and 8).

### 3.2 Cable-stayed Ting Kau Bridge (TKB)

The TKB as illustrated in Fig. 8 is a cable-stayed bridge with two main spans of 448 m and 475 m respectively, and two side spans of 127 m each. It has single-deck carrying a dual four-lane expressway and three single-leg towers supporting the deck. In the bridge, each of the two halves of the deck consists of two longitudinal steel girders along the deck edges with steel cross-girders and a concrete slab on top. Every third cross-girder is extended continuously to the central cross-girder to connect the two carriageways. The four main longitudinal girders carry the main load effects from the deck to the stay cables. The deck is supported only at the central tower in the longitudinal direction. In the transverse direction, the deck is supported at all three towers. On both ends of the bridge, the deck is vertically connected by rocker bearings into the northern end pier and the southern end abutment. The critical problem of a multi-span cable-stayed bridge is the stabilization of the central tower. Therefore, longitudinal stabilizing cables, with the length up to 464.6 m, are installed to stabilize the central tower. Transverse stabilizing cables are also used to strengthen each tower in sway direction. There are totally 456 cables including 384 main stay cables in four cable planes, 64 transverse stabilizing cables and 8 longitudinal stabilizing cables.

A precise 3D FEM containing 5,581 elements and 2,901 nodes has been developed for the TKB by using the commercial ABAQUS software. The modeling is based on the same criteria as for the modeling of the TMB. In this FEM, the bridge deck is modeled by membrane/shell elements to account for the horizontal thrust ability, while its bending stiffness is represented in the steel grid structure as nominal flanges of the longitudinal girders and cross-girders. The towers are modeled as Timoshenko's beam elements. The geometric distances between cable ends and the cross-

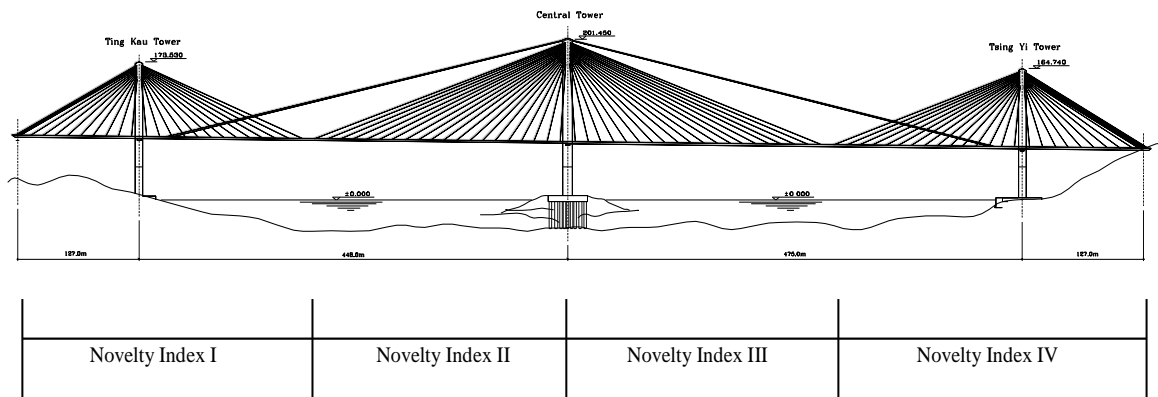


Fig. 8 Cable-stayed Ting Kau Bridge (TKB)

section centroids of the deck and towers are represented by rigid bars. A key issue in the modeling of the TKB is how to model the total 456 cables to realize a compromise between the model scale (system degrees of freedom) and the model accuracy (reflecting the influence of cable vibration). After a comparison between adopting a multi-element cable system for all the cables and modeling the main stay cables, longitudinal stabilizing cables and transverse stabilizing cables as single-element cable systems in turn, a hybrid-element strategy is finally used in the modeling where the longitudinal stabilizing cables are modeled by a multi-element cable system while the other cables are modeled by a single-element cable system.

Modal analysis with the FEM shows that the modal frequencies of the TKB are closely spaced and the frequencies of the first 100 modes are less than 1.0 Hz. The vibration modes of the TKB can be classified into the following categories: (i) global vertical bending modes, (ii) global lateral bending modes, (iii) global torsional modes, (iv) cable local out-of-plane modes, and (v) cable local in-plane modes. The first three categories are global modes while the latter two are local modes of the longitudinal stabilizing cables. All the global modes are accompanied with local vibration components of the cables to some extent. With the above modal classification, five ANNs configured in terms of the improved novelty index are formulated for damage occurrence detection of the TKB: the 1st ANN with a node structure 11-6-6-11 has its input layer being the modal frequencies of the first 11 the global vertical bending modes (category (i)); the 2nd ANN with a node structure 6-4-4-6 has its input layer being the modal frequencies of the first 6 global lateral bending modes (category (ii)); the 3rd ANN with a node structure 12-9-9-12 has its input layer being the modal frequencies of the first 12 global torsional modes (category (iii)); the 4th ANN with a node structure 18-11-11-18 has its input layer being the modal frequencies of the first 18 cable local out-of-plane modes (category (iv)); and the 5th ANN with a node structure 13-9-9-13 has its input layer being the modal frequencies of the first 13 cable local in-plane modes (category (v)).

A series of 'measured' modal frequencies of the healthy structure are obtained by adding to the computed modal frequencies from the FEM normally distributed random noises with zero mean and 0.005 variance, which are used to train the five ANNs and obtain the novelty index sequences in the training phase. A total of eleven damage cases, as listed in Table 5, are introduced for the damage detection simulation study. The modal frequencies for each damage case are calculated by incurring the simulated damage in the FEM, which are then corrupted by normally distributed

Table 5 Simulated damage cases for TKB

Case No.	Description
1	20% tension force reduction of one longitudinal stabilizing cable
2	20% tension force reduction of two longitudinal stabilizing cables
3	90% tension force loss of one main stay cable
4	90% tension force loss of two main stay cables
5	90% tension force loss of four main stay cables
6	Damage of a longitudinal bearing at the central tower
7	Damage of an anchorage bearing at the Tsing Yi abutment
8	Damage of one longitudinal girder section
9	Damage of two longitudinal girder sections and two cross-girder sections
10	Damage of one connecting cross-girder
11	Damage of two connecting cross-girders

random noises with zero mean and 0.005 variance to generate the ‘measured’ data in the damage state. By presenting these data into the trained ANNs, the novelty index sequences in the testing phase are obtained.

Figs. 9 and 10 show the novelty indices for Case 1 and Case 7 evaluated on the five ANNs. In Case 1 (the damage is simulated by a 20% reduction of tension force in a longitudinal stabilizing cable), the novelty index sequences in the testing phase deviate significantly from the sequences in the training phase when evaluated on the 1st, 3rd and 4th ANNs, unambiguously signaling the damage occurrence. The damage occurrence cannot be flagged when evaluated on the 2nd and 5th ANNs. In Case 7 (the damage is incurred in an anchorage bearing at the Tsing Yi abutment), the novelty index evaluated on the 1st ANN unambiguously signals the occurrence of damage, with the deviation being larger than the threshold. When evaluated on the 2nd ANN, the novelty index sequences in the training and testing phases are clearly distinguishable although the deviation is less than the threshold. The damage occurrence cannot be flagged when evaluated on the 3rd, 4th and 5th ANNs, where the novelty index sequences in the two phases are indistinguishable. It is observed that in the noise level of 0.005 variance ( $\pm 1.5\%$  maximum error), the novelty index cannot indicate the occurrence of damage in some cases. Table 6 summarizes the performance of the five ANNs in damage occurrence detection for all eleven cases.

Table 7 lists the evaluated maximum frequency change ratios of the first 125 modes of the bridge corresponding to the eleven damage cases. It is found that when the maximum frequency change ratio  $\gamma$  is less than 0.4%, the damage occurrence cannot be flagged by the proposed novelty index (Cases 3, 4, 5, 8 and 10). When the maximum frequency change ratio  $\gamma$  is between 0.4% and 1.0% (Cases 9 and 11), the damage is just detectable with a weak alarming signature. The novelty index can unambiguously alarm the damage states when the maximum frequency change ratio  $\gamma$  is greater than 1.0% (Cases 1, 2, 6 and 7). Under the identical noise level (0.005 variance), the minimum frequency change ratio for the TKB (0.4%) which makes damage detectable by the proposed novelty detection technique is slightly different from that for the TMB (0.3%); whereas they are fairly consistent with each other. The difference between them is primarily attributed to different structural type and scale (and therefore different redundancy degree) between the two bridges, which results in different modal sensitivity of the two bridges to damage in the same extent.

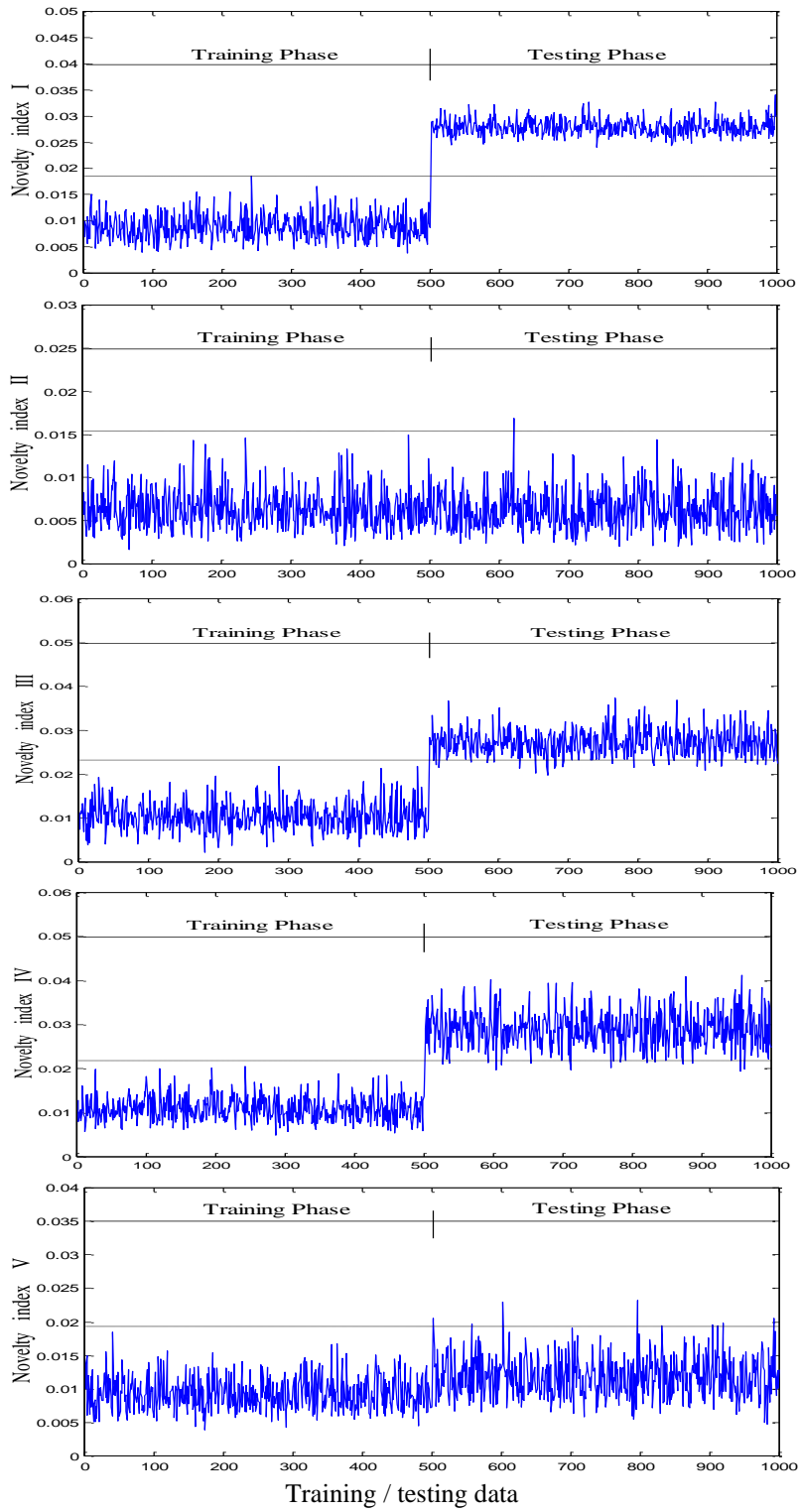


Fig. 9 Novelty index evaluated on the testing data in Case 1 of TKB

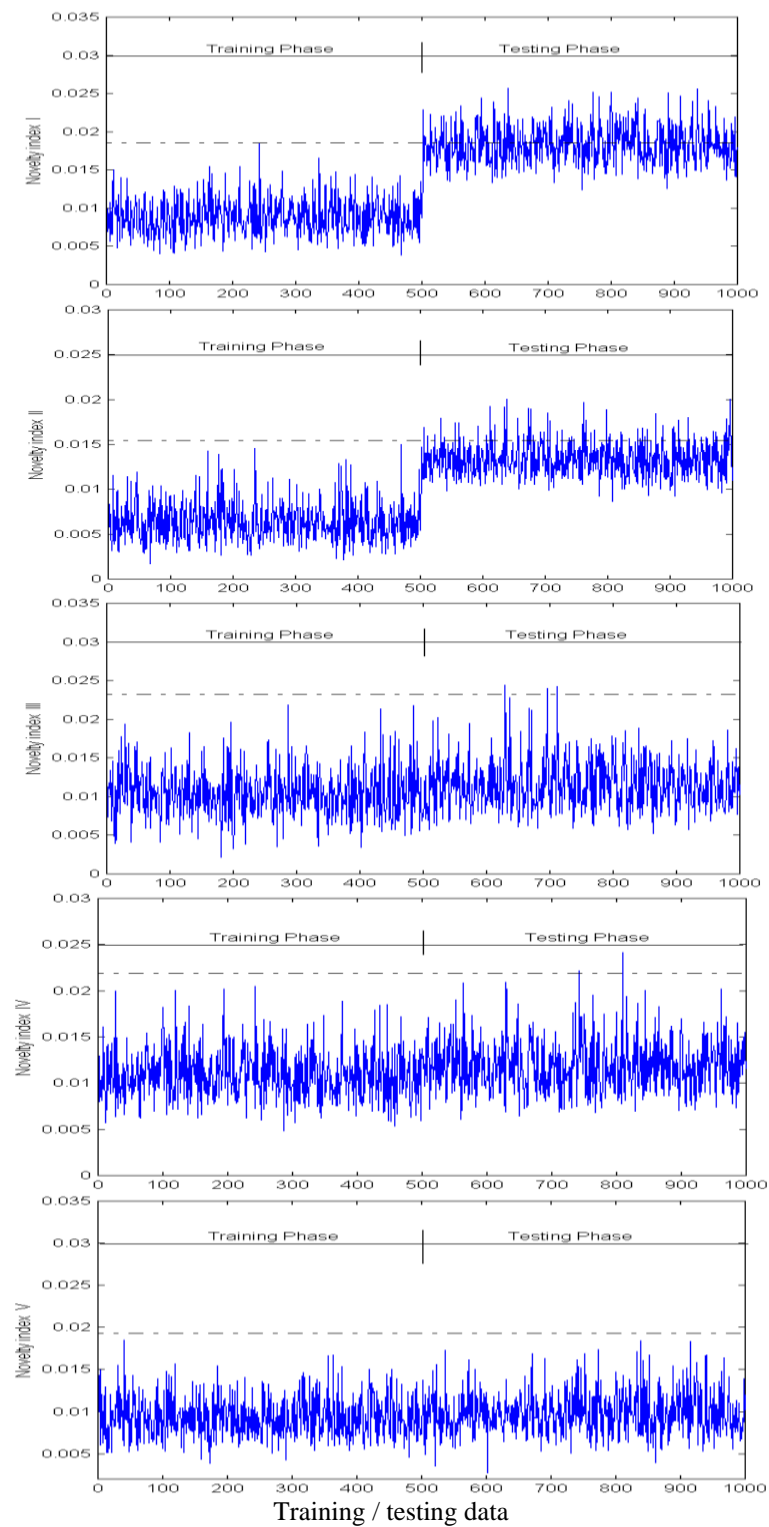


Fig. 10 Novelty index evaluated on the testing data in Case 7 of TKB

Table 6 Structure of ANNs for TKB and damage detection results

ANN No.	Input and output vectors	Node structure	Damage cases successfully detected
I	11 modal frequencies of category (i)	11-6-6-11	Cases 1, 2, 6, 7, 9 and 11
II	6 modal frequencies of category (ii)	6-4-4-6	Cases 6 and 7
III	12 modal frequencies of category (iii)	12-9-9-12	Cases 1, 2 and 6
IV	18 modal frequencies of category (iv)	18-11-11-18	Cases 1 and 2
V	13 modal frequencies of category (v)	13-9-9-13	Case 2

Table 7 Damage-caused maximum frequency change ratio for TKB

Case No.	Case 1	Case 2	Case 3	Case 4	Case 5	Case 6
$\gamma$ (%)	3.7015	3.7926	0.0268	0.0537	0.1348	6.4518
Case No.	Case 7	Case 8	Case 9	Case 10	Case 11	
$\gamma$ (%)	2.9527	0.3968	0.7044	0.3749	0.9570	

#### 4. Identification of damage region by multi-novelty indices

For model-free damage detection methods, using only the measured modal frequencies is impossible to locate damage. In this study, we extend the novelty detection technique to diagnose the damage region without need of structural model. Multi-novelty indices constructed in terms of modal flexibility coefficients are developed for this purpose. Following this approach, the bridge is partitioned into a set of structural regions and it is assumed that there are vibration transducers at each region. For each structural region, an ANN is formulated by taking the modal flexibility coefficients as input feature, which are calculated using the global modal frequencies and a few localized modeshape components measured from the sensors deployed within this region. The damage region is signaled by the corresponding novelty index if it exhibits a drift from the training phase to the testing phase. The modal flexibility matrix  $[F]$  can be calculated from the modal frequency matrix  $[A]$  and the mass-normalized modeshape matrix  $[\Phi]$  as follows

$$[F] = [\Phi]^T [A]^{-1} [\Phi] \quad (8)$$

where the elements of the modal flexibility matrix  $[F]$  are obtained by

$$F_{ij} = \begin{cases} \sum_r \frac{1}{\omega_r^2} \phi_{ir} \phi_{jr} & i \neq j \\ \sum_r \frac{1}{\omega_r^2} \phi_{ir}^2 & i = j \end{cases} \quad (9)$$

If the novelty index sequence in the testing phase deviates from that in the training phase, the occurrence of structural damage/anomaly is flagged; if they are indistinguishable, no damage is signaled.

In practice, only a limited number of modes and a few modeshape components can be measured for a complex civil structure. An advantage of using modal flexibility is that the modal flexibility matrix of a structure can be accurately estimated by considering only a few low-order

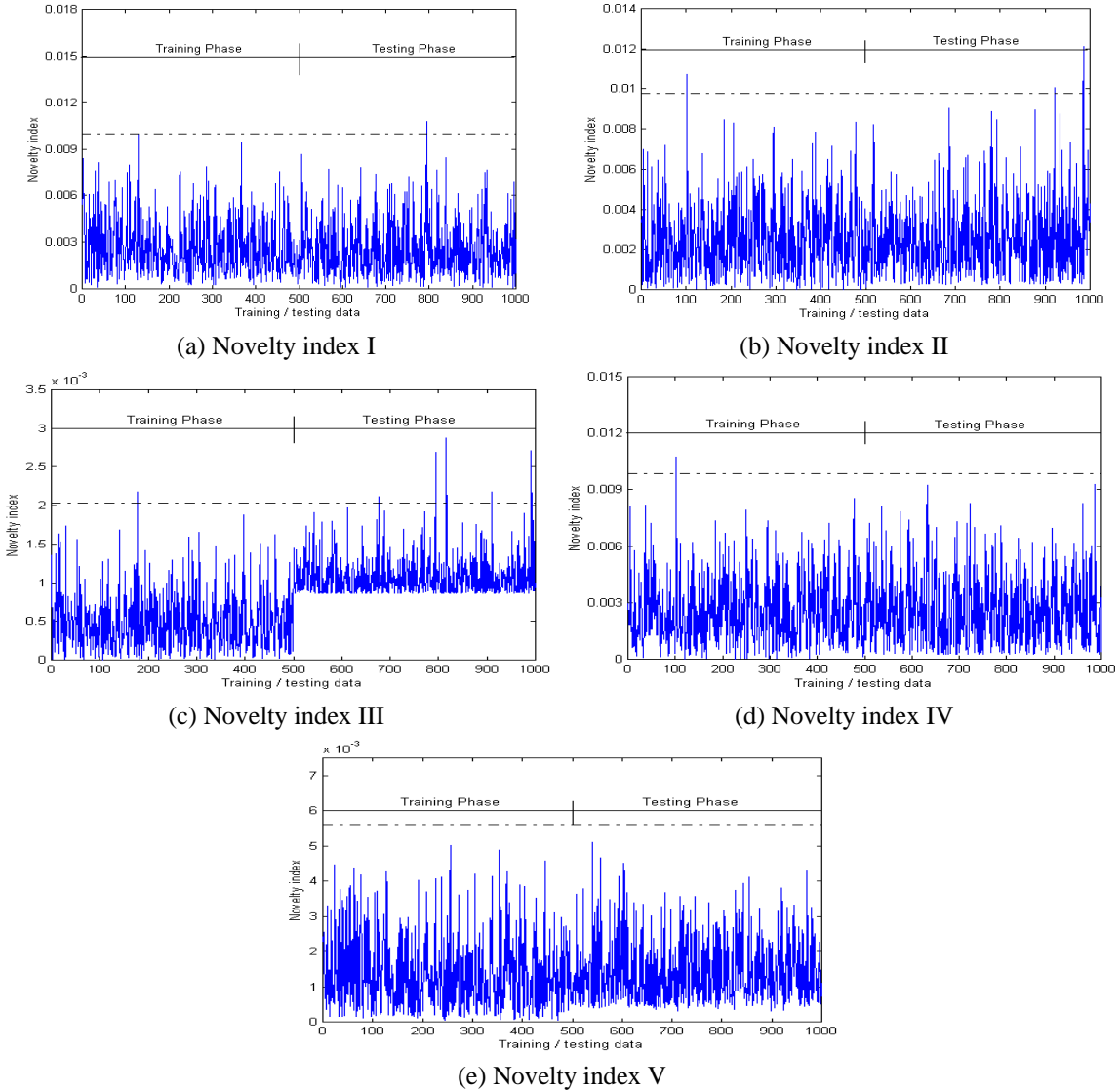


Fig. 11 Multi-novelty indices using modal flexibility for damage localization (Case 11 of TMB)

modes, because the modal contribution to flexibility decreases as frequency increases. Therefore, using a limited number of modes and a few modeshape components, the flexibility matrix can be expressed as the following approximate equation (Ni *et al.* 2008)

$$[\mathbf{F}]_{p \times p} \approx [\mathbf{\Phi}]_{p \times m}^T [\mathbf{A}]_{m \times m} [\mathbf{\Phi}]_{m \times p} \tag{10}$$

where  $m$  denotes the number of measured or selected modes; and  $p$  denotes the number of measured modeshape components (measured DOFs). Both  $m$  and  $p$  are substantially smaller than the total number of DOFs in the analytical model,  $n$ . In the present study, only the diagonal terms of  $[\mathbf{F}]_{p \times p}$  are used.

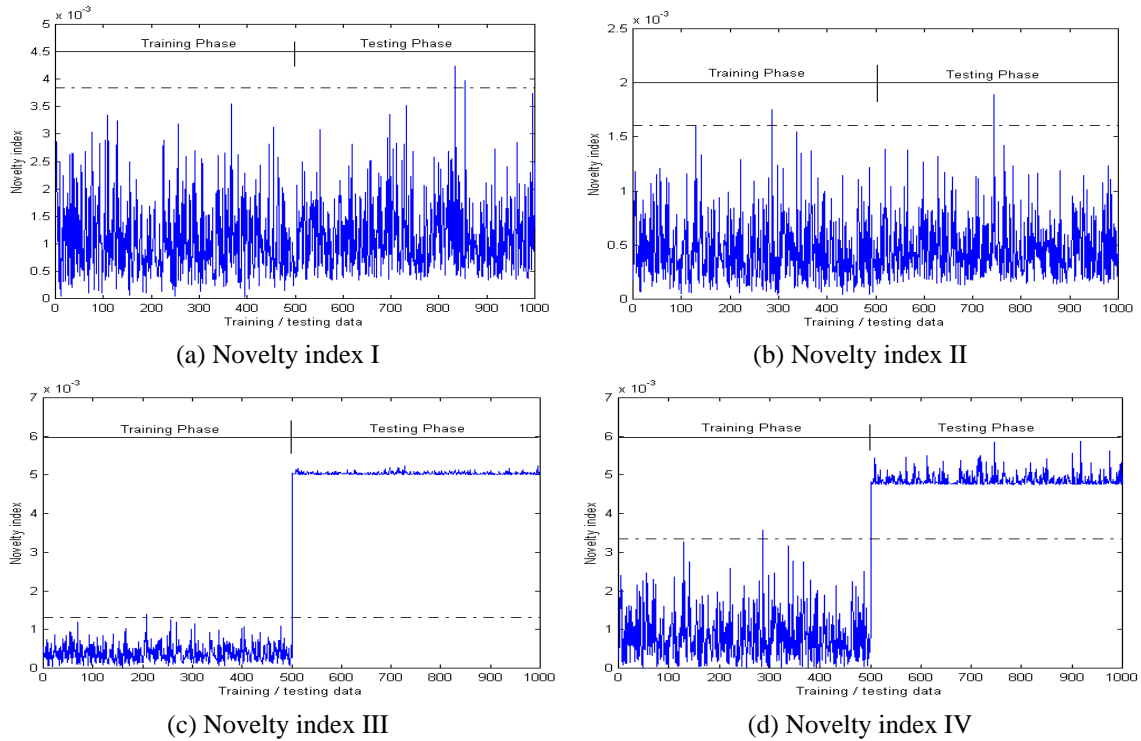


Fig. 12 Multi-novelty indices using modal flexibility for damage localization (Case 10 of TKB)

The diagonal components of the measurement-derived modal flexibility matrix are used instead of the modal frequencies as input feature to train an ANN and to obtain a novelty index for each region. As such, multi-novelty indices are formulated for different regions. The damage region is signaled by the corresponding novelty index that displays drift from the training phase to the testing phase. In the following, we demonstrate the applicability of the proposed method for structural damage region identification by taking the TMB and TKB as examples.

#### 4.1 Suspension Tsing Ma Bridge (TMB)

We consider only the main span deck of the TMB in this example. As illustrated in Fig. 2, the main span of the TMB is partitioned into five regions. It is assumed that for each region five modal components are measured. Then the modal flexibility values (diagonal components) at the five nodes for each region are computed by taking the first five global modes, and further corrupted independently with normally distributed random noises with zero mean and 0.005 variance to generate the ‘measured’ modal flexibility sequences. Five ANNs, one for each region, are configured with a node structure 5-3-3-5 for damage region identification. Each ANN is trained using only the five modal flexibility sequences obtained in the relevant region. The previous Case 11 of the TMB is examined here (the damage is assumed by removing two longitudinal bottom chords near the mid-span). Fig. 11 shows the novelty detection results by means of the multi-novelty indices in this case. In the structural regions I, II, IV and V, no damage is signaled because the novelty index sequences in training phase do not deviate from their

counterparts in testing phase. For the structural region III, the novelty index sequence in the training phase evidently deviates from that in the testing phase (although the deviation is less than the threshold), indicating damage occurrence in this region. Indeed, the true damage occurs at the mid-span deck section within the region III.

#### 4.2 Cable-stayed Ting Kau Bridge (TKB)

We partition the TKB into four regions as shown in Fig. 8. It is assumed that for each region six modal components of the nodes at girders and longitudinal stabilizing cables are measured. The modal flexibility values (diagonal components of the flexibility matrix) at the six nodes for each region are computed by taking the first five global modes. These analytical values are corrupted independently with normally distributed random noises with zero mean and 0.005 variance to generate the 'measured' modal flexibility sequences. Four ANNs, one for each region, are configured with a node structure 6-4-4-6 for damage region identification. Each ANN is trained using only the six modal flexibility sequences obtained in the relevant region. The previous Case 10 for the TKB is examined here (the damage is assumed by losing the stiffness of a cross-girder). The damage location is nearly in the middle of the Tsing Yi main span (at the deck section between the outermost cable stretching from the central tower and the outermost cable stretching from the Tsing Yi tower). Fig. 12 shows the novelty detection results by using the multi-novelty indices. The novelty indices indicate no damage in the regions I and II, and alarm damage in the regions III and IV. In fact, the true damage occurs at the intersection between the regions III and IV, and therefore the novelty indices indicate the damage simultaneously at the two regions.

## 5. Conclusions

This paper presents a feasibility study on the detection of damage occurrence and damage region by using an improved novelty index formulated in terms of auto-associative neural networks (ANNs) and a multi-novelty index technique, both being free of structural model. For the detection of damage occurrence, only measured modal frequencies are required to train ANNs and to formulate the improved novelty index for damage alarming. For the identification of damage region, it is required to measure a few modeshape components for each region as well. The modal flexibility values (diagonal components of the flexibility matrix) obtained from the measured modal frequencies and incomplete modeshape components are used to train ANNs and to formulate multi-novelty indices for damage localization. The proposed techniques are verified through numerical simulations by using FEMs of the suspension Tsing Ma Bridge (TMB) and the cables-stayed Ting Kau Bridge (TKB). According to the modal classification, five ANNs are configured for the TMB and TKB, respectively, to identify the occurrence of structural damage. The multi-novelty indices for damage region identification are constructed using five modeshape components at each region and the modal frequencies of the first five global modes in the TMB case and using six modeshape components at each region and the modal frequencies of the first five global modes in the TKB case. The numerical simulations with the aid of FEMs enable the consideration of different types and extents of damage and help to reveal the relationship between damage detectability by the proposed novelty detection technique and the damage-caused modal frequency change ratio. The following conclusions are drawn from the present study:

1. For the TMB, when only modal frequencies are used and normally distributed random noises

with zero mean and 0.005 variance ( $\pm 1.5\%$  maximum error) are considered, the ANN-based novelty detectors are able to unambiguously alarm the damage states if the damage-caused maximum modal frequency change ratio is greater than 1.0%. When the maximum modal frequency change ratio is between 0.3% and 1.0%, the damage is just detectable with a weak alarming signature. The occurrence of damage cannot be flagged if the maximum modal frequency change ratio is less than 0.3%;

2. For the TKB, when only natural frequencies are used and normally distributed random noises with zero mean and 0.005 variance ( $\pm 1.5\%$  maximum error) are considered, the ANN-based novelty detectors are able to unambiguously alarm the damage states if the damage-caused maximum modal frequency change ratio is greater than 1.0%. When the maximum modal frequency change ratio is between 0.4% and 1.0%, the damage is just detectable with a weak alarming signature. The occurrence of damage cannot be flagged if the maximum modal frequency change ratio is less than 0.4%;

3. The multi-novelty indices in terms of modal flexibility values derived using the measured modal frequencies and incomplete modeshape components can provide identification of the damage region in the TMB and TKB without need of structural model. However, the proposed method is operational on the assumption that there exist vibration transducers in each region to measure a few modal components. The proposed method also requires a series of measurements of the modal data in both healthy and damage states.

## Acknowledgments

The work described in this paper was supported by a grant from the Research Grants Council of the Hong Kong Special Administrative Region, China (Project No. PolyU 5224/13E).

## References

- Abdelghani, M. and Friswell, M.I. (2007), "Sensor validation for structural systems with multiplicative sensor faults", *Mech. Syst. Signal Pr.*, **21**, 270-279.
- Aktan, A.E., Chase, S., Inman, D. and Pines, D.D. (2001), "Monitoring and managing the health of infrastructure systems", *Health Monitoring and Management of Civil Infrastructure Systems*, Proceedings of SPIE Vol. 4337, SPIE, Eds. S.B. Chase, A.E. Aktan, Bellingham, Washington, USA.
- Brownjohn, J.M.W. (2007), "Structural health monitoring of civil infrastructure", *Phil. Tran. Roy. Soc. A*, **365**, 589-622.
- Catbas, F.N. (2009), "Structural health monitoring: applications and data analysis", *Structural Health Monitoring of Civil Infrastructure Systems*, Eds. V.M. Karbhari, F. Ansari, Woodhead Publishing, Cambridge, UK.
- Chan, T.H.T., Ni, Y.Q. and Ko, J.M. (1999), "Neural network novelty filtering for anomaly detection of Tsing Ma Bridge cables", *Structural Health Monitoring 2000*, Ed. F.K. Chang, Technomic Publishing Co., Lancaster, Pennsylvania.
- Dan, D., Sun, L., Yang, Z. and Xie, D. (2014), "The application of a fuzzy inference system and analytical hierarchy process based online evaluation framework to the Donghai Bridge health monitoring system", *Smart Struct. Syst.*, **14**, 129-144.
- DeWolf, J.T., Lauzon, R.G. and Culmo, M.P. (2002), "Monitoring bridge performance", *Struct. Hlth. Monit.*, **1**, 129-138.

- Fujino, Y., Siringoringo, D.M. and Abe, M. (2009), "The needs for advanced sensor technologies in risk assessment of civil infrastructures", *Smart Struct. Syst.*, **5**, 173-191.
- Glisic, B., Inaudi, D. and Casanova, N. (2009), "SHM process - lessons learned in 250 SHM projects", *Proceedings of the 4th International Conference on Structural Health Monitoring and Intelligent Infrastructure*, Zurich, Switzerland.
- Hernandez-Garcia, M.R. and Masri, S.M. (2008), "Multivariate statistical analysis for detection and identification of faulty sensors using latent variable methods", *Adv. Sci. Tech.*, **56**, 501-507.
- Hinton, G.E. (1989), "Connectionist learning procedures," *Artif. Intel.*, **40**, 185-234.
- Hua, X.G., Ni, Y.Q., Chen, Z.Q. and Ko, J.M. (2009), "Structural damage detection of cable-stayed bridges using changes in cable forces and model updating", *J. Struct. Eng.*, ASCE, **135**, 1093-1106.
- Ko, J.M. and Ni, Y.Q. (2005), "Technology developments in structural health monitoring of large-scale bridges", *Eng. Struct.*, **27**, 1715-1725.
- Ko, J.M., Ni, Y.Q. and Chan, T.H.T. (1999), "Dynamic monitoring of structural health in cable-supported bridges", *Smart Structures and Materials 1999: Smart Systems for Bridges, Structures, and Highways*, Ed. S.C. Liu, SPIE Vol. 3671, Bellingham, Washington, USA.
- Ko, J.M., Ni, Y.Q., Wang, J.Y., Sun, Z.G. and Zhou, X.T. (2000), "Studies of vibration-based damage detection of three cable-supported bridges in Hong Kong", *Proceedings of the International Conference on Engineering and Technological Sciences 2000 - Session 5: Civil Engineering in the 21st Century*, Eds. J. Song, G. Zhou, Science Press, Beijing, China.
- Ko, J.M., Ni, Y.Q., Zhou, H.F., Wang, J.Y. and Zhou, X.T. (2009), "Investigation concerning structural health monitoring of an instrumented cable-stayed bridge", *Struct. Infrast. Eng.*, **5**, 497-513.
- Ko, J.M., Sun, Z.G. and Ni, Y.Q. (2002), "Multi-stage identification scheme for detecting damage in cable-stayed Kap Shui Mun Bridge", *Eng. Struct.*, **24**, 857-868.
- Kullaa, J. (2010), "Sensor validation using minimum mean square error estimation", *Mech. Syst. Signal Pr.*, **24**, 1444-1457.
- Kullaa, J. (2011), "Distinguishing between sensor fault, structural damage, and environmental or operational effects in structural health monitoring", *Mech. Syst. Signal Pr.*, **25**, 1508-1526.
- Lau, C.K., Mak, W.P.N., Wong, K.Y., Chan, W.Y.K. and Man, K.L.D. (1999), "Structural health monitoring of three cable-supported bridges in Hong Kong," *Structural Health Monitoring 2000*, Ed. F.K. Chang, Technomic Publishing Co., Lancaster, Pennsylvania.
- Liao, W.Y., Ni, Y.Q. and Zheng, G. (2012), "Tension force and structural parameter identification of bridge cables", *Adv. Struct. Eng.*, **15**, 983-995.
- Ni, Y.Q., Ko, J.M. and Zheng, G. (2002), "Dynamic analysis of large-diameter sagged cables taking into account flexural rigidity", *J. Sound Vib.*, **257**, 301-319.
- Ni, Y.Q., Wong, K.Y. and Xia, Y. (2011), "Health checks through landmark bridges to sky-high structures", *Adv. Struct. Eng.*, **14**, 103-119.
- Ni, Y.Q., Xia, Y., Liao, W.Y. and Ko, J.M. (2009a), "Technology innovation in developing the structural health monitoring system for Guangzhou New TV Tower", *Struct. Control Hlth. Monit.*, **16**, 73-98.
- Ni, Y.Q., Zhou, H.F., Chan, K.C. and Ko, J.M. (2008), "Modal flexibility analysis of cable-stayed Ting Kau Bridge for damage identification", *Comput. Aid. Civil Infrast. Eng.*, **23**, 223-236.
- Ni, Y.Q., Zhou, H.F. and Ko, J.M. (2009b), "Generalization capability of neural network models for temperature-frequency correlation using monitoring data", *J. Struct. Eng.*, ASCE, **135**, 1290-1300.
- Oh, C.K., Sohn, H. and Bae, I.H. (2009), "Statistical novelty detection within the Yeongjong suspension bridge under environmental and operational variations", *Smart Mater. Struct.*, **18**, 125022.
- Ou, J., and Li, H. (2009), "Structural health monitoring research in China: trends and applications", *Structural Health Monitoring of Civil Infrastructure Systems*, Eds. V.M. Karbhari, F. Ansari, Woodhead Publishing, Cambridge, UK.
- Pandey, A.K. and Biswas, M. (1994), "Damage detection in structures using changes in flexibility", *J. Sound Vib.*, **169**, 3-17.
- Petsche, T., Marcantonio, A., Darken, C., Hanson, S.J., Kuhn, G.M., and Santoso, I. (1996), "A neural

- network autoassociator for induction motor failure prediction”, *Advances in Neural Information Processing Systems 8*, Eds. D.S. Touretzky, M.C. Mozer, M.E. Hasselmo, The MIT Press, Cambridge, Massachusetts, USA.
- Rumelhart, D.E., Hinton, G.E. and Williams, R.J. (1986), “Learning internal representations by error propagation”, *Parallel Distributed Processing: Explorations in the Microstructure of Cognition*, Eds. D.E. Rumelhart, J.L. McClelland, The MIT Press, Cambridge, Massachusetts, USA, **1**, 318-362.
- Sim, P.L.J., Worden, K. and Manson, G. (2004), “An adaptive structural health monitoring strategy using novelty detectors”, *Proceedings of the 2nd European Workshop on Structural Health Monitoring*, Eds. C. Boller, W.J. Staszewski, DEStech Publications, Lancaster, Pennsylvania, USA, 633-641.
- Sohn, H., Worden, K. and Farrar, C.R. (2002), “Statistical damage classification under changing environmental and operational conditions”, *J. Intel. Mater. Syst. Struct.*, **13**, 561-574.
- Teng, J., Lu, W., Wen, R. and Zhang, T. (2015), “Instrumentation on structural health monitoring systems to real world structures”, *Smart Struct. Syst.*, **15**, 151-167.
- Toksoy, T. and Aktan, A.E. (1994), “Bridge-condition assessment by modal flexibility”, *Exper. Mech.*, **34**, 271-278.
- Wang, J.Y., Ko, J.M. and Ni, Y.Q. (2000), “Modal sensitivity analysis of Tsing Ma Bridge for structural damage detection”, *Nondestructive Evaluation of Highways, Utilities, and Pipelines IV*, Eds. A.E. Aktan, S.R. Gosselin, SPIE Vol. 3995, 300-311.
- Wang, M.L. and Yim, J. (2010), “Sensor enriched infrastructure system”, *Smart Struct. Syst.*, **6**, 309-333.
- Wong, K.Y. (2004), “Instrumentation and health monitoring of cable-supported bridges”, *Struct. Control Hlth. Monit.*, **11**, 91-124.
- Worden, K. (1997), “Structural fault detection using a novelty measure”, *J. Sound Vib.*, **201**, 85-101.
- Yan, A.M., De Boe, P. and Golinval, J.C. (2004), “Structural damage diagnosis by Kalman model based on stochastic subspace identification”, *Struct. Hlth. Monit.*, **3**, 103-119.
- Ye, X.W., Ni, Y.Q., Wai, T.T., Wong, K.Y., Zhang, X.M. and Xu, F. (2013), “A vision-based system for dynamic displacement measurement of long-span bridges: algorithm and verification”, *Smart Struct. Syst.*, **12**, 363-379.
- Yun, C.B., Lee, J.J. and Koo, K.Y. (2011), “Smart structure technologies for civil infrastructures in Korea: recent research and applications”, *Struct. Infrastr. Eng.*, **7**, 673-688.
- Zhou, H.F., Ni, Y.Q. and Ko, J.M. (2011a), “Eliminating temperature effect in vibration-based structural damage detection”, *J. Eng. Mech.*, ASCE, **137**, 785-796.
- Zhou, H.F., Ni, Y.Q. and Ko, J.M. (2011b), “Structural damage alarming using auto-associative neural network technique: exploration of environment-tolerant capacity and setup of alarming threshold”, *Mech. Syst. Signal Pr.*, **25**, 1508-1526.